

## Supplementary Materials

### **Subtractive manufacturing with swelling induced stochastic folding of sacrificial materials for fabricating complex perfusable tissues in multi-well plates**

Shravanthi Rajasekar<sup>1,\*</sup>, Dawn S. Y. Lin<sup>1,\*</sup>, Feng Zhang<sup>2,\*</sup>, Alexander Sotra<sup>1,2</sup>, Alex Boshart<sup>3,4</sup>, Sergi Clotet-Freixas<sup>3,4</sup>, Amy Liu<sup>5</sup>, Jeremy A. Hirota<sup>2,6,7</sup>, Shinichiro Ogawa<sup>8,9</sup>, Ana Konvalinka<sup>3,4,9,10,11</sup>, and Boyang Zhang<sup>1,2,\*\*</sup>

<sup>1</sup>Department of Chemical Engineering, McMaster University, 1280 Main Street West, Hamilton, ON, L8S 4L8, Canada

<sup>2</sup>School of Biomedical Engineering, McMaster University, 1280 Main Street West, Hamilton, ON, L8S 4L8, Canada

<sup>3</sup>Advanced Diagnostics, Toronto General Hospital Research Institute, University Health Network, Toronto, Ontario, Canada

<sup>4</sup>Renal Transplant Program, Soham and Shaila Ajmera Family Transplant Centre, University Health Network, Toronto, Ontario, Canada

<sup>5</sup>Faculty of Health Sciences, McMaster University 1280 Main Street West, Hamilton, ON, L8S 4L8, Canada

<sup>6</sup>Department of Medicine, Division of Respiriology, McMaster University, 1200 Main St W Hamilton, ON, L8N 3Z5, Canada

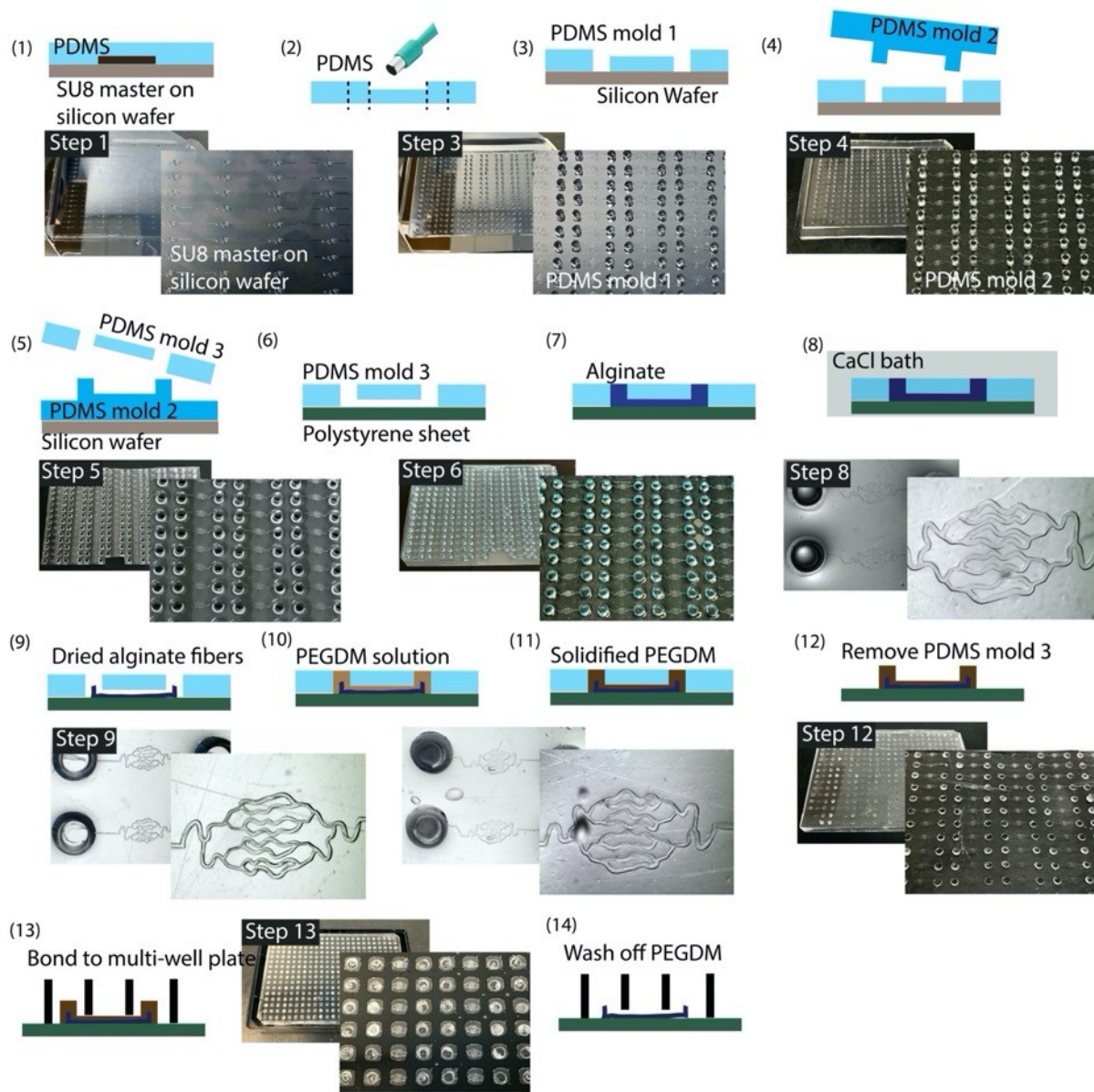
<sup>7</sup>Firestone Institute for Respiratory Health, St. Joseph's Hospital, Hamilton, ON, L8N 4A6, Canada.

<sup>8</sup>McEwen Stem Cell Institute, University Health Network, 101 College St, MaRS Center, Toronto, Ontario, M5G 1L7 Canada

<sup>9</sup>Department of Laboratory, Medicine and Pathobiology, University of Toronto, 101 College St, MaRS Center, Toronto, Ontario, M5G 1L7 Canada

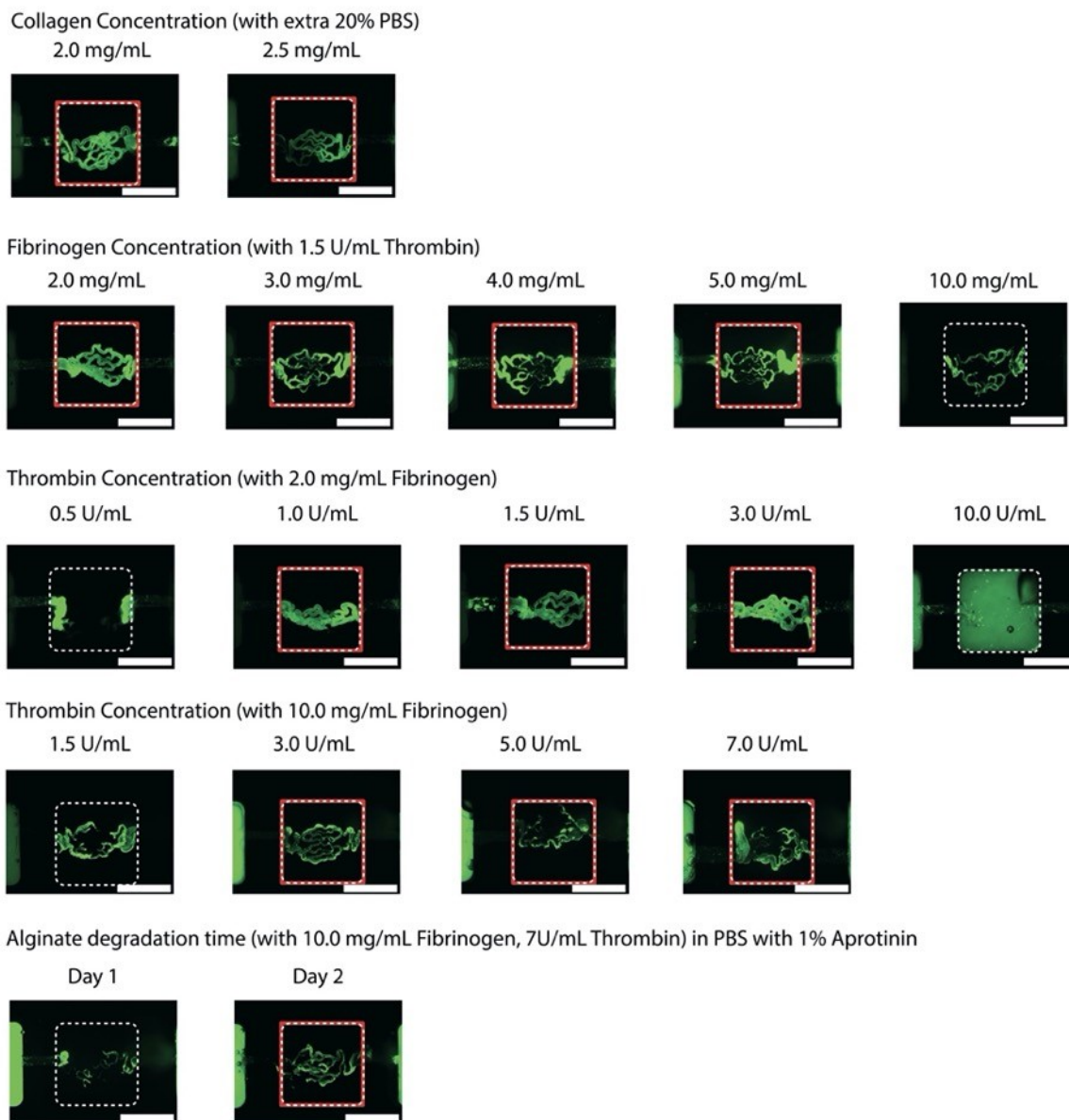
<sup>10</sup>Department of Medicine, Division of Nephrology, University Health Network, Toronto, Ontario, Canada

<sup>11</sup>Institute of Medical Science, University of Toronto, Toronto, Ontario, Canada

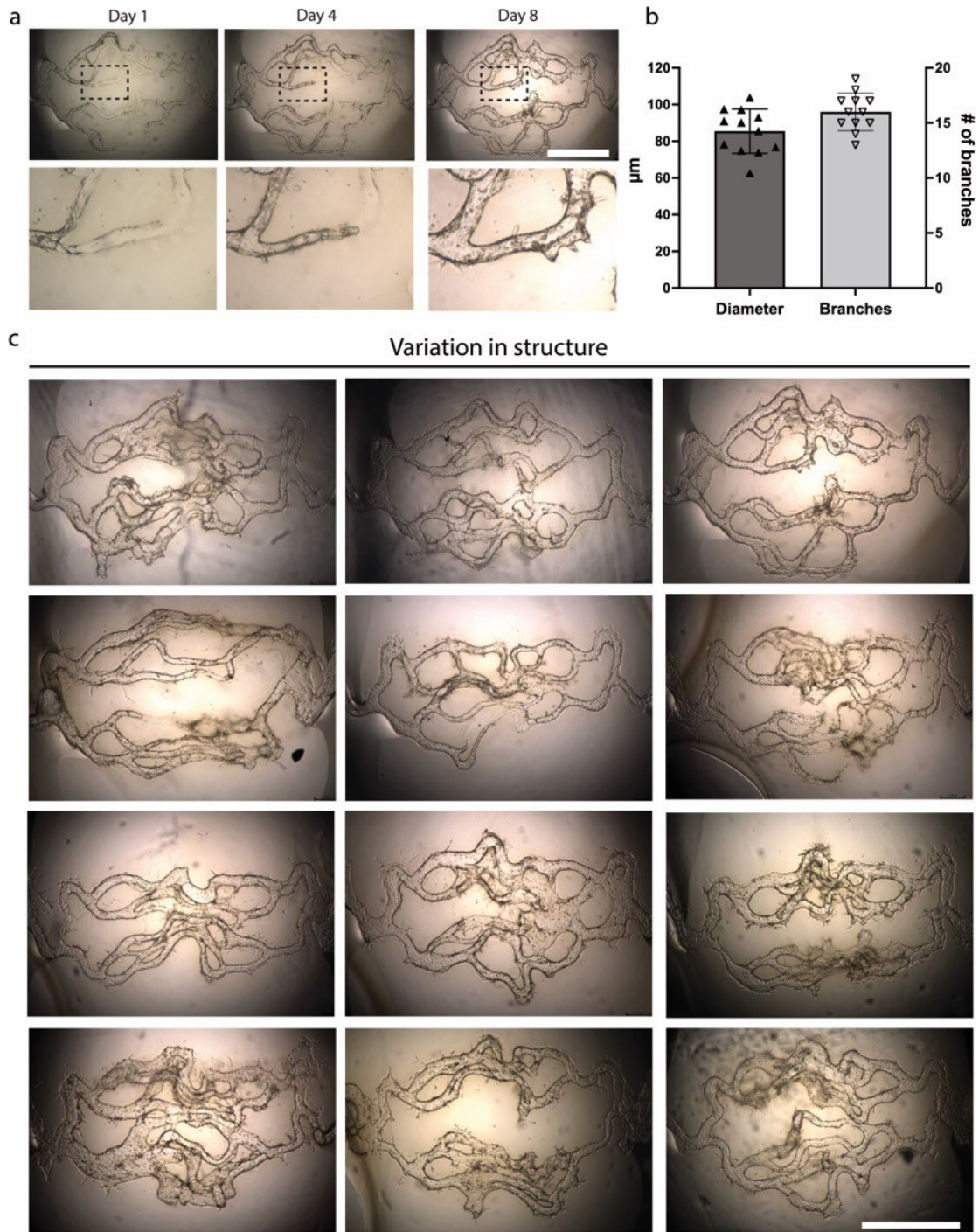


**Supplementary Figure 1. Step-by-step fabrication of AngioPlate-384.** First, using standard photolithography, we fabricated a PDMS mold with various patterns connected to an inlet and outlet well. The mold was then capped onto a polystyrene sheet to form an array of micro-channel networks. The networks were loaded with 3 wt.% alginate solution. Next, the entire mold was immersed in a calcium bath (1 mM), where calcium ions gradually diffused from the inlet and outlet wells into the alginate solution within the network, cross-linking the alginate overnight. With this approach, we were able to pattern 128 independent alginate fiber networks in the format of a 384-well plate. PEGDM solution was injected into the channels in the same way to encapsulate the alginate fiber to facilitate alginate release and to create the inlet/outlet channels. Finally, the polystyrene sheet patterned with alginate and PEGDM was assembled onto the base of a bottomless 384-well plate, encasing and sealing the alginate networks with a high viscosity PDMS glue.

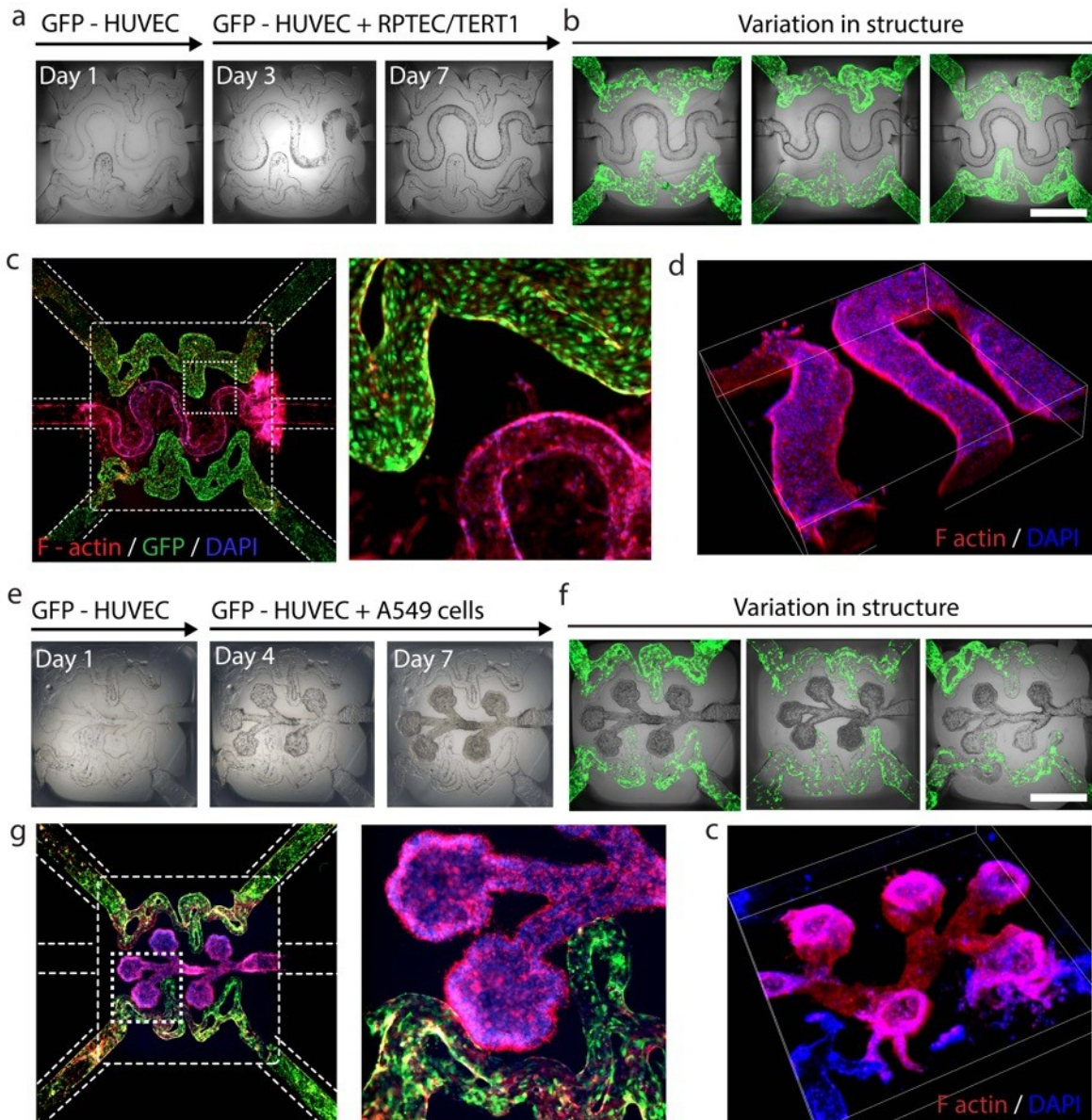




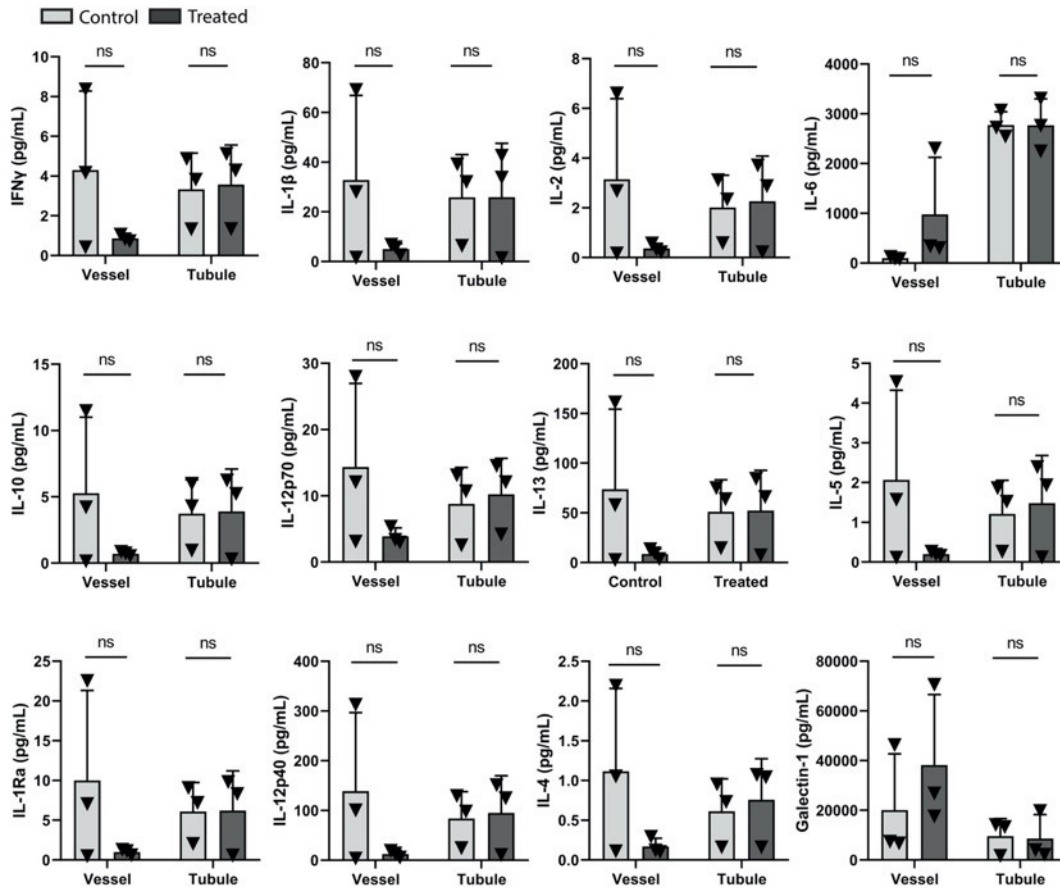
**Supplementary Figure 2. Optimization of hydrogel matrix cross-linking condition for network formation.** Fluorescent images of networks perfused with 1  $\mu$ m fluorescent particles (green) under various gelling conditions in both collagen-based gel and fibrin-based gel. Red boxes label the good conditions that resulted in the formation of complete perfusable networks. Scale bar, 2mm.



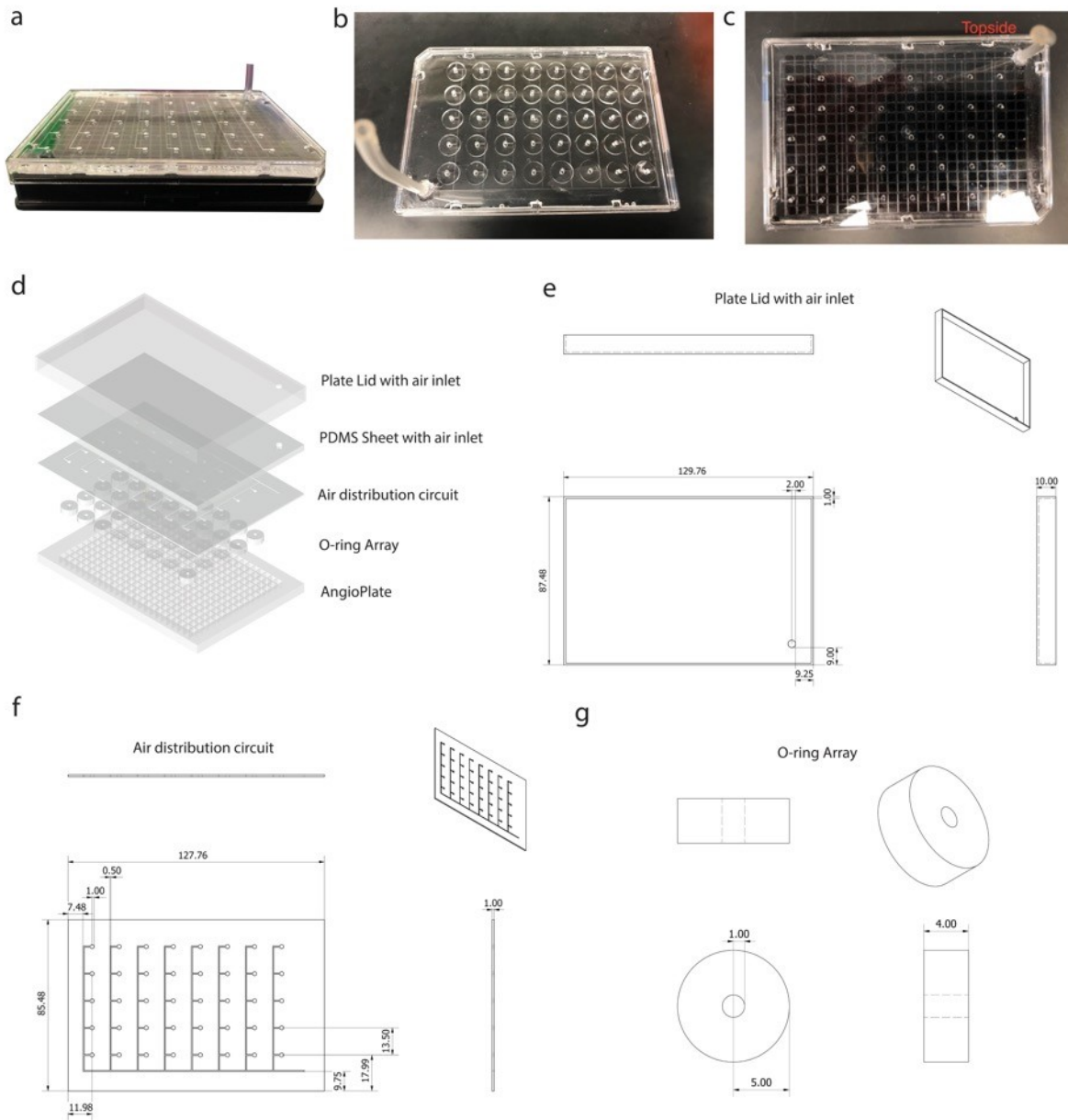
**Supplementary Figure 3. Structural variation of vasculature in AngioPlate.** **a**, Brightfield time-lapse images of networks seeded with human endothelial cells. Scale bar 1mm. **b**, Quantification of variation in vasculatures structure. n=12. **c**, Variation in the network structures from 12 different wells. Scale bar 1mm.



**Supplementary Figure 4. AngioPlate-Lung and Kidney.** **a**, Time-lapse brightfield images of a vascularized proximal tubule complex. Endothelial cells were seeded on day 0 and tubular cells were seeded on day 3. **b**, Variation in the structure of the vascular proximal tubule complex resulting from alginate folding. Scale bar 1 mm. **c-d**, Fluorescent images of vascular proximal tubule complex stained for F-actin (red) and DAPI (blue). **e**, Time-lapse brightfield images of a vascularized alveoli terminal. Endothelial cells were seeded on day 0 and Alveolar cells were seeded on day 3. **f**, Variation in the structure of vascularized alveoli terminal resulting from alginate folding. Scale bar 1 mm. **g-h**, Fluorescent images of a vascularized alveoli terminal stained for F-actin (red) and DAPI (blue).



**Supplementary Figure 5. Cytokine assay of inflammatory kidney.** Cytokine analysis of media perfusates from tissues treated with or without TNF- $\alpha$ , n=3. Statistical significance was determined using one-way ANOVA and one-way ANOVA on ranks with the Holm-Sidak method. ns indicates not significantly different. \*P $\leq$ 0.05 \*\*P $\leq$ 0.01 \*\*\*P $\leq$ 0.001



**Supplementary Figure 6. Mechanical actuation lid design, dimension and assembly.** **a**, Image of the plate lid on an AngioPlate. **b**, Top-down view of the actuation lid. **c** Top-down view of the actuation lid on our device without the O-ring array to show alignment with the wells in an AngioPlate. **d**, Assembly of different parts in the actuation lid. **e-g**, Dimensions and design of parts of the plate actuation lid, including the air distribution circuit and the o-rings. All labels are shown in millimeters.

**Supplementary Video 1.** Swelling and shape changing alginate fibers on AngioPlate  
**Supplementary Video 2.** Mechanical actuation of terminal alveoli on AngioPlate